

# A metal-to-insulator transition in cut-wire-grid metamaterials in the terahertz region

Keisuke Takano,<sup>1,a)</sup> Kyoji Shibuya,<sup>1</sup> Koichi Akiyama,<sup>2</sup> Takeshi Nagashima,<sup>1</sup> Fumiaki Miyamaru,<sup>3,4</sup> and Masanori Hangyo<sup>1</sup>

<sup>1</sup>*Institute of Laser Engineering, Osaka University, 2-6 Yamadaoka, Suita, Osaka 565-0871, Japan*

<sup>2</sup>*Advanced Technology R&D Center, Mitsubishi Electric Corporation, 8-1-1 Tsukaguchi-Honmachi, Amagasaki, Hyogo 661-8661, Japan*

<sup>3</sup>*Department of Physics, Faculty of Science, Shinshu University, 3-1-1 Asahi, Matsumoto, Nagano 390-8621, Japan*

<sup>4</sup>*PRESTO, Japan Science and Technology Agency, 2-1-1 Katahira, Aoba, Sendai 980-8577, Japan*

(Received 13 October 2009; accepted 7 December 2009; published online 27 January 2010)

Metamaterials with metallic wire-grid structures support extremely low frequency plasmons and their electromagnetic responses exhibit metallic characteristics described by the Drude model. In this paper, we have investigated the electromagnetic responses of the wire-grid structures in the terahertz frequency range when periodic and random cuts are introduced in the wires. It is found experimentally that the wire-grid structures exhibit a transition from a metallic response of negative permittivity to an insulators-like response of large positive permittivity at terahertz frequencies when small cuts are introduced in the wires. It is also revealed from the finite-difference time-domain simulation that such a transition is accompanied by an enhancement of the electric fields in the cuts, which is applicable to practical technologies. © 2010 American Institute of Physics. [doi:10.1063/1.3284958]

## I. INTRODUCTION

The metamaterials of periodic arrays of metallic thin wires (wire-grid structures) are the simplest and most popular structures to design the negative permittivity.<sup>1-6</sup> The wire-grid structures behave like diluted metals for the electromagnetic waves polarized parallel to the wires. The effective plasma frequency is depressed by the artificial structures to the extremely low frequency region. The electromagnetic waves polarized parallel to the wires are blocked below the effective plasma frequency (cutoff frequency) and transmitted above the effective plasma frequency. In the microwave and terahertz regions, such properties of the metal wire-grids have been used as polarizers and high-pass filters for a long time.<sup>7-9</sup>

In the case of one-dimensional (1D) wire-grid arrays [Fig. 1(a)], the effective permittivity for TE waves (incident electric fields parallel to the wires) is described by

$$\epsilon = \epsilon_0 \left( 1 + \frac{1}{i\omega\epsilon_0 p d Z_w} \right), \tag{1}$$

where  $Z_w = i\omega L + R$  is series of effective total inductive impedance  $i\omega L$  and resistance  $R$  per unit length,<sup>2</sup> and  $\epsilon_0$  is the permittivity of vacuum. Here, the parallel capacitance between the adjacent wires are neglected, and the cross section area of the unit cell is assumed to be  $pd$ , where  $p$  and  $d$  are the period and thickness of the wires as shown in Fig. 1. The effective permittivity is negative below an effective plasma frequency so that the wire-grid structures exhibit plasmonic responses. Comparing Eq. (1) to the Drude model,

$$\epsilon = \epsilon_0 \left( 1 - \frac{\omega_p^2}{\omega(\omega - i\tau^{-1})} \right), \tag{2}$$

where  $\omega_p$  is the plasma frequency and  $\tau$  is the relaxation time, the effective plasma frequency and relaxation time are obtained as

$$\omega_{p,\text{eff}} = \sqrt{\frac{1}{\epsilon_0 p d L}}, \quad \tau_{\text{eff}} = \frac{L}{R}. \tag{3}$$

In Refs. 2-4, the authors described that if periodic cuts are inserted in the wires [Fig. 1(b)], the negative permittivity metamaterials change into artificial dielectrics. Awai and co-workers<sup>10,11</sup> have also proposed this structure as a high permittivity artificial dielectric metamaterial. Recently, several similar structures are used to fabricate negative refractive index media and metamaterial absorbers.<sup>12,13</sup> By introducing the cuts, capacitive impedance  $1/i\omega C$  is added into the impedance,

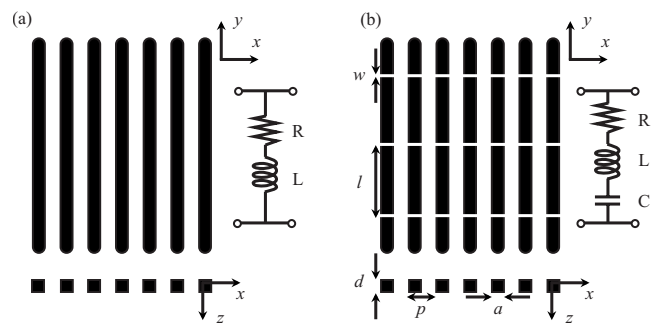


FIG. 1. Schematic diagrams of (a) wire-grid structure and (b) cut-wire-grid structure. Equivalent circuits are also shown.

<sup>a)</sup>Electronic mail: ktakano@ile.osaka-u.ac.jp.

$$Z_w = i\omega L + \frac{1}{i\omega C} + R. \quad (4)$$

Equations (1) and (4) predict that the electromagnetic responses of the wire-grid structures exhibit a transition from metallic one to insulating one below the  $LC$  resonance frequency  $1/2\pi\sqrt{LC}$  by introducing cuts. Additionally, the transition happens abruptly even if the inserted cut width is very small because the inductive impedance decreases with decreasing  $\omega$  and the capacitive impedance increases with  $\omega^{-1}$  in the frequency region much lower than the  $LC$  resonance frequency. The permittivity becomes a positive constant value at very low frequencies,

$$\varepsilon \approx \varepsilon_0 \left( 1 + \frac{C}{\varepsilon_0 p d} \right). \quad (5)$$

The drastic change of the electromagnetic responses is desirable for an electromagnetic modulation or sensing using metamaterials.<sup>14–16</sup>

In this paper, we demonstrate the drastic transitions from the metals to insulators in the metamaterials with the cut-wire-grid structures experimentally in the terahertz frequency range. Additionally, the case of random cuts is discussed from the standpoint of the comparison of the cut-wire-grid metamaterials with the real materials such as conducting polymers. The finite-difference time-domain (FDTD) simulations reveal that the electric fields concentrate in the small cuts at low frequencies. This electric field confinement is useful for improving the sensitivity of terahertz sensors and the enhancement of nonlinear optical effects.

## II. FABRICATION OF SAMPLES AND TERAHERTZ TIME-DOMAIN SPECTROSCOPY

Printing using a general-purpose printer (ALPS MD-5500) with spot-color ink imitating a gold color (ALPS MDC-FMG) is a simple and useful method for fabricating two-dimensional (2D) metallic structures.<sup>17</sup> The spot-color ink exhibits metallic responses in the terahertz frequency region. It is possible to print arbitrary 2D patterns on papers with the maximum resolution of about 100  $\mu\text{m}$ . The ink thickness is about 2.5  $\mu\text{m}$ .

The transmission spectra of the printed 2D patterns were measured by the terahertz time-domain spectroscopy (terahertz-TDS) system. The transmittance  $T$  and phase shift  $\phi$  at each frequency are obtained simultaneously by the terahertz-TDS measurements. Assuming the permeability  $\mu = 1$ , the optical constants are calculated from the following relationship between the complex amplitude transmission coefficient  $\sqrt{T}e^{i\phi}$  and the optical constants in a two-layer system (ink and paper in our case, see Fig. 2),<sup>18,19</sup>

$$\begin{aligned} \sqrt{T}e^{i\phi} &= \frac{E_3^+}{E_0^+} \\ &= \frac{t_{01}t_{12}t_{23}e^{i(k_1d_1+k_2d_2)-ik_3(d_1+d_2)}}{1 + r_{01}r_{12}e^{2ik_1d_1} + r_{01}r_{23}e^{2i(k_1d_1+k_2d_2)} + r_{12}r_{23}e^{2ik_2d_2}}. \end{aligned} \quad (6)$$

Figure 3 shows the real parts of the relative permittivity and

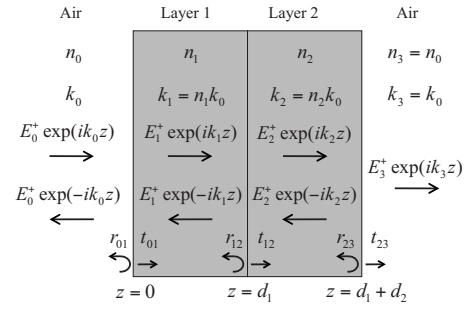


FIG. 2. Electromagnetic wave propagation in a two-layer system.  $E_i^+$ ,  $E_i^-$ ,  $n_i$ , and  $k_i$  ( $i=0, 1, 2$ , and  $3$ ) are amplitudes of the electric fields, refractive index, and wavenumber in each layer. The superscripts + and – denote the positive and negative directions.  $t_{ij}$  and  $r_{ij}$  are the Fresnel transmission and reflection coefficients. The subscript  $ij$  denotes the interfaces between the layers  $i$  and  $j$ . Equation (6) is derived from the boundary conditions at  $z=0, d_1$ , and  $d_1+d_2$  (Ref. 19).

conductivity of the ink daubed all over the substrate paper. The thickness of the paper  $d_2$  is 0.07 mm and the refractive index  $n_2$  is  $1.5+i0.05$ , which is obtained by the terahertz-TDS measurement. The responses of the metallic ink are fitted well to the Drude model [Eq. (2)] with  $\nu_p = \omega_p/2\pi = 9.1$  THz and  $\tau = 0.1$  ps. The ink behaves like the Drude metals in the terahertz region. All structures examined in this paper were fabricated by this method.

## III. A TRANSITION FROM METALS TO INSULATORS IN CUT-WIRE-GRID METAMATERIALS

The cut-wire-grid structures were printed on the substrate papers and their transmittance and phase shift spectra were measured by the terahertz-TDS system. A schematic and photograph are shown in Fig. 1 and the inset of Fig. 4, respectively. The dimensions of the structures are indicated in the caption of Fig. 4. The transmittance and phase shift

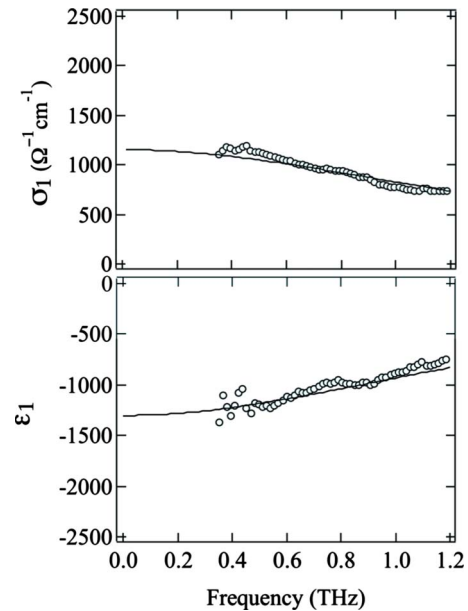


FIG. 3. (Color online) Real parts of the relative permittivity and conductivity of the metallic ink on the paper. Open circles are obtained by the terahertz-TDS measurements. Solid lines are fitted to the Drude model whose plasma frequency is  $\nu_p = \omega_p/2\pi = 9.1$  THz and the relaxation time is  $\tau = 0.1$  ps.

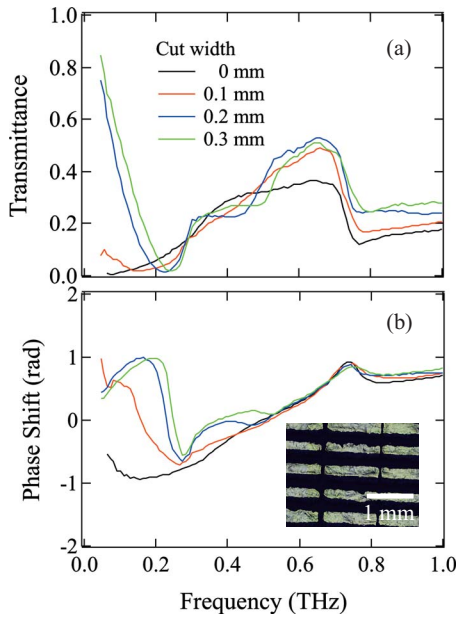


FIG. 4. (Color online) Transmittance and phase shift of the cut-wire-grid structures printed on the substrate papers. Their characteristic dimensions are the wire period  $p=0.4$  mm, wire width  $d=0.2$  mm, cut period  $l=1$  mm, and cut with  $w=0, 0.1, 0.2,$  and  $0.3$  mm. The substrate papers have the thickness of  $0.07$  mm and the refractive index of  $1.5+i0.05$ . The ink thickness is about  $2.5 \mu\text{m}$ . The inset photograph shows a typical picture of the sample with the cut width of  $0.1$  mm

spectra for the TE waves are shown in Fig. 4. Without the cuts in the wires, it shows a typical wire-grid response.<sup>6,17</sup> The dips at around  $0.75$  THz in the transmission spectra correspond to the frequency of the first order diffraction from the wire period  $\nu_d=c/p$ , where  $c$  is the speed of light in vacuum. By introducing the cuts in the wires, stop bands attributed to the  $LC$  resonance appear around  $0.2$  THz.<sup>3</sup> We observe the drastic increase in the transmittance and the change from negative values to positive ones in the phase shift at the frequencies below the stop bands; they are more remarkable for larger cut widths. Because the capacitance is dominant in the impedance of the series of  $L$ ,  $C$ , and  $R$  below the  $LC$  resonance, the electromagnetic waves can transmit through the open circuit consisted of the capacitance of the cuts.<sup>7</sup>

Assuming the printed pattern as a uniform layer with the thickness of  $2.5 \mu\text{m}$  in the lateral directions (layer 1 in Fig. 2), the effective permittivity and conductivity are deduced using Eq. (6). Ikonen *et al.*<sup>4</sup> discussed that how the effective thickness of the wire-grid structures should be chosen. For the case of the single-layered wire-grid, the effective thickness is chosen to be the wire diameter (corresponding to the realistic thickness of the single wire-grid) so that a homogeneous medium having the effective permittivity and thickness almost reproduces the transmittance and reflectance of the single-wire grid structure. Following this, we use the thickness of ink  $2.5 \mu\text{m}$  as layer 1. However, it is noted that the effective permittivity is not meaningful for a multilayered wire-grid.

Figure 5 indicates the real parts of the effective relative permittivity and conductivity of the cut-wire-grid structures. It must be noted that these effective values are meaningful

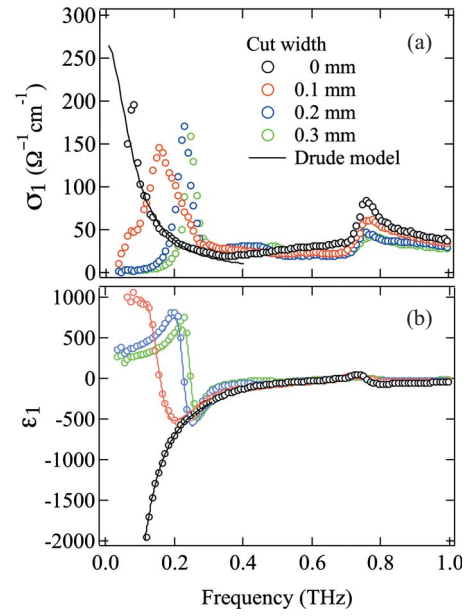


FIG. 5. (Color online) Effective conductivity and relative permittivity deduced from the transmittance and phase shift in Fig. 4. Open circles are the experimental data. Solid curves in the permittivity spectra are the fitted curves to Eqs. (1) and (4). The fitting parameters are listed in Table I.

below  $0.3$  THz where the diffraction waves due to the periodic cuts do not exist. For the cut width  $w=0$  mm (no cuts), the responses ( $\sigma_1$  and  $\epsilon_1$ ) are fitted to the Drude model with  $\nu_p=\omega_p/2\pi=0.99$  THz and  $\tau=2$  ps. When the cuts are introduced in the wires, the permittivity and conductivity exhibit the Lorentz-type dispersions described by the following equation:

$$\epsilon = \epsilon_0 \left( 1 + \frac{1/\epsilon_0 p d L}{1/LC - \omega^2 + i\omega R/L} \right), \quad (7)$$

which is derived by substituting Eq. (4) into Eq. (1). In the vicinity of the  $LC$  resonance the permittivity exhibits large positive and negative values.

Below the  $LC$  resonance frequency, the introduction of the cuts changes the effective permittivity from large negative values to large positive values. This means that the cuts in the wires change the cut-wire structures from metallic to insulating metamaterials. The conductivity in the low frequency limit  $\sigma(0)$  becomes 0 by the introduction of the cuts [Fig. 5(a)]. It reflects that the dc current in the wires is blocked by the cuts, even though the cut width is much smaller than the incident wavelength. By fitting the effective permittivity to Eq. (7) in the frequency range upto  $0.4$  THz, the effective  $LCR$  parameters are estimated [Fig. 5(b)]. The fitting parameters are listed in Table I. The responses without

TABLE I. Fitting parameters in Fig. 5(b).

Cut width (mm)	L ( $10^{-7}$ H/m)	C ( $10^{-18}$ Fm)	R ( $10^4 \Omega$ m)
0	0.78	>1000	3.66
0.1	1.13	7.67	8.20
0.2	1.92	2.55	6.05
0.3	2.44	1.70	6.38

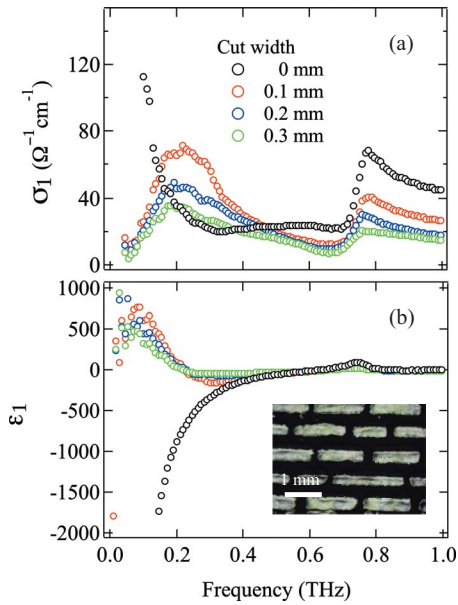


FIG. 6. (Color online) Effective conductivity and relative permittivity of the random cut-wire-grid metamaterials. The inset photo is the case of  $w = 0.1$  mm.

the cuts mean that the capacitance value is assumed to be infinity. The effective capacitance decreases by two orders of magnitude when the small cuts are introduced. The introduction of the capacitive impedance is obviously a dominant factor for the change of the electromagnetic responses. In contrast, owing to the small volume of the cuts, effective inductance and resistance are less sensitive to the cuts. Thus, the introduction of the cuts can change the electromagnetic responses below the  $LC$  resonance frequency without changing the responses above the  $LC$  resonance frequency as discussed in Ref. 3.

#### IV. RANDOM CUT-WIRE-GRID METAMATERIALS

It is interesting to compare the responses of the cut-wire-grid structures to those of real materials. Recently, Lee *et al.*<sup>20</sup> reported an achievement of truly metallic conducting polymers. The conductivity  $\sigma(\omega)$  of their high-quality polyaniline samples is typical of conventional metals, which fits to the Drude model. However, the most conducting polymers exhibit a decrease in the conductivity as the frequency decreases in the low frequency region owing to the disorder-induced localization of the charge carriers. These polymers behave like disordered metals near the metal-insulator transition.<sup>21–24</sup> The disorders exist randomly in the materials. Figure 6 shows the effective conductivity and relative permittivity of the cut-wire-grid structures in which the cuts are introduced randomly in the wires. The average period of the cuts is 1 mm. The randomness broadens the  $LC$  resonance and the conductivity shows a broad peak. The introducing of the cuts causes a transition from the metallic to insulating responses as well as the periodic cases.

A number of reports successfully explained the behavior of  $\sigma(\omega)$  of the conducting polymers using inhomogeneous model. One of the disorders in the metallic polymers arises from the inhomogeneities in the mesoscopic structures. In

the inhomogeneous disorder model, the conductivity is modeled as series of the conductivity in the metallic region and disordered region. The Drude model describes the conductivity in the metallic regions  $\sigma_m(\omega)$  in the polymer. In contrast, the conductivity in the inhomogeneous disorders is modeled as  $\sigma_b(\omega) = \rho^{-1} + i\omega\varepsilon_b$  where,  $\rho$  is the resistivity and  $i\omega\varepsilon_b$  is the admittance in the inhomogeneous barrier (insulating) regions with the permittivity  $\varepsilon_b$ . The macroscopic conductivity of the polymers is represented by  $\sigma^{-1}(\omega) = [g_m\sigma_m(\omega)]^{-1} + [g_b\sigma_b(\omega)]^{-1}$ , where  $g_m$  and  $g_b$  are the geometrical factors.<sup>21,22</sup> The conducting polymers are metallic in the high frequency region because the Drude responses are dominant. However, in the low frequency region, the polymers become insulators because the admittance of the disorder regions is dominant. Above perspective on the conducting polymers is almost the same as the treatment of the cut-wire-grid structures in this paper. Actually, Fig. 6 is very similar to the optical responses of the conducting polymers in the references. We believe that the metal-insulator transition observed for the conducting polymer samples is explained partly by the structure change shown here.

#### V. FDTD SIMULATION

To characterize the electromagnetic wave propagation in the cut-wire-grid structures, we performed the FDTD simulations using a commercial software package.<sup>25</sup> The simulation model and calculated transmission spectra are shown in Fig. 7. The ink thickness of our simulation model is thicker than the experimental samples owing to the limit of our computer power. However, the transmittance shows good agreements with the experiments. For the cut width of  $w = 0.1$  mm, the electric field distribution on the  $x$ - $y$  plane, which is in the paper and  $10 \mu\text{m}$  away from the metallic ink was calculated (Fig. 8). As the frequency decreases, the electric fields are concentrated in the cuts. Although the wavelength is about 100 times larger than the cut width at 0.03 THz, the transmittance is larger than 0.5 and the electric field distribution is highly concentrated in the cuts. The field intensity in the cuts is more than 40 times larger than that of the incident waves. It is inferred that at the frequencies much lower than the  $LC$  resonance, the transmittance and the electric field enhancements become much higher.

The electric field concentration in the low frequency region can be understood by regarding the cuts as parallel-plate waveguides. Because the cutoff frequency does not exist in the metallic parallel-plate waveguide for the incident waves polarized perpendicular to the plate, the electromagnetic waves whose wavelength is much longer than the width of the metallic parallel-plates can exist in the waveguide as the TEM mode.<sup>26,27</sup> Thus, the long wavelength terahertz waves can be squeezed in the cuts as seen in Fig. 8(a). Amazingly, the terahertz waves can be squeezed into the slit even if the slit width is several tens of nanometer.<sup>28,29</sup> In Ref. 29, the terahertz waves are focused and strongly enhanced in the  $\lambda/30\,000$  width gold slit. Their experiments imply that the metallic response of the wire-grid structures become the insulating one by the introducing the cuts with the width of only several tens of nanometers.

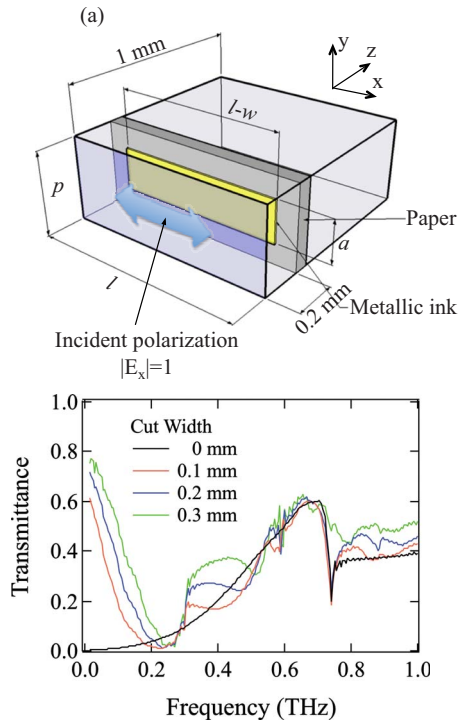


FIG. 7. (Color online) (a) Unit cell of the FDTD simulation model. We used the periodic boundary conditions in the  $x$  and  $y$  directions. The incident waves are linearly polarized along the  $x$  direction and have the amplitude of unity. The period of the cuts  $l$  is 1 mm, wire period  $p$  is 0.4 mm, and wire width  $a$  is 0.2 mm. The substrate paper has the refractive index of  $1.5 + i0.05$  and thickness of 0.07 mm. The metallic ink is defined as a Drude metal whose plasma frequency and collision time are obtained from Fig. 3. The thickness of the ink is 0.01 mm. (b) Change of the transmission spectrum of the cut-wire-grid structures when the cut width  $w$  is changed from 0 to 0.3 mm.

It is noted that this kind of electric field enhancements is effective over a wide frequency range from microwave to optical regions because of the scaling law for Maxwell equations. Miyazaki and Kurokawa<sup>30–32</sup> succeeded in squeezing visible light into the metal-insulator-metal nanocavities whose thickness and length is several nanometer and several tens of nanometer, respectively. The fundamental principle of their field confinement for the optical frequency range is same as that for the cut-wire-grid structures mentioned here.

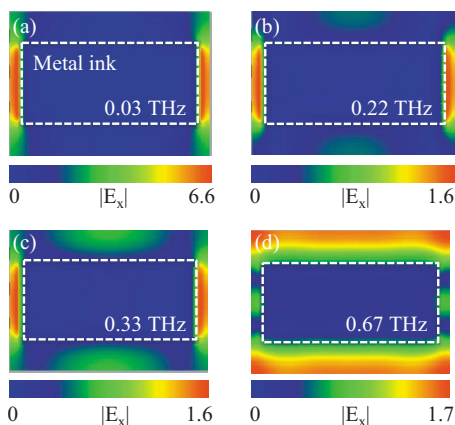


FIG. 8. (Color online) Electric field distributions in the cut wire-grid structures. The observation areas are placed on the  $x$ - $y$  plane in the paper and 10  $\mu\text{m}$  away from the metallic ink.

If the cut-wire-grids are scaled down to exhibit the  $LC$  resonances at the few hundred nanometers incident wavelengths, the visible light is concentrated in the few nanometer cuts. Such electric field confinement in the cut-wire-grid structures is also important for the spatially selective enhancement of nonlinear optical effects<sup>33,34</sup> or sensing applications for small amount samples.

## VI. CONCLUSION

We demonstrated the sharp transition from the plasmonic to insulating responses in the metamaterials having the cut-wire-grid structures. The wire-grid structures behave as Drude-like metals for the electromagnetic waves polarized parallel to the metal wires. By introducing the cuts in the wires, the capacitive impedance drastically changes the electromagnetic responses. Especially in the low frequency region, the effective conductivity and permittivity exhibit a transition from the metallic to insulating responses owing to the capacitive impedance of the cuts. We believe that the transitions of the cut-wire-grid metamaterial responses imitate partly those of the real materials such as conducting polymers.

The drastic spectral changes by the small structural differences are attractive for the terahertz applications such as the intensity modulation devices. If the cut-wire structures are made on semiconductor substrates, the terahertz transmittance can be controlled by irradiating the gap with light or applying voltage.<sup>14,15</sup> Additionally, the FDTD simulations reveal that the electric fields are concentrated in the cuts whose widths are much smaller than the wavelength in the low frequency region. Recently, some high power terahertz radiation sources are becoming popular.<sup>35–37</sup> The field concentration by metallic structures presented in this paper is effective for further enhancement of the fields to induce nonlinear effects in the terahertz region.

## ACKNOWLEDGMENTS

This work has been partly supported by a Grant-in-Aid for Scientific Research for Priority Area “Strong Photon-Molecule Coupling Fields for Chemical Reactions” (Grant No. 20043019) from The Ministry of Education, Culture, Science, and Technology, Japan and a Grant-in-Aid for Scientific Research (A) (Grant No. 20246022) from Japan Society of Promotion of Science. F.M. is also supported by the Murata Science Foundation and the Konica Minolta Imaging Science Foundation.

<sup>1</sup>S. A. Ramakrishna and T. M. Grzegorzczak, *Physics and Applications of Negative Refractive Index Materials* (CRC, Boca Raton, 2008).

<sup>2</sup>S. I. Maslovski, S. A. Tretyakov, and P. A. Belov, *Microwave Opt. Technol. Lett.* **35**, 47 (2002).

<sup>3</sup>P. A. Belov, C. R. Simovski, and S. A. Tretyakov, *Phys. Rev. E* **66**, 036610 (2002).

<sup>4</sup>P. Ikonen, E. Saenz, R. Gonzalo, C. Simovski, and S. Tretyakov, *Metamaterials* **1**, 89 (2007).

<sup>5</sup>J. Pendry, A. Holden, W. Stewart, and I. Youngs, *Phys. Rev. Lett.* **76**, 4773 (1996).

<sup>6</sup>B. Pradarutti, C. Rau, G. Torosyan, R. Beigang, and K. Kawase, *Appl. Phys. Lett.* **87**, 204105 (2005).

<sup>7</sup>R. Ulrich, *Infrared Phys.* **7**, 37 (1967).

<sup>8</sup>C. L. Mok, W. G. Chambers, T. J. Parker, and A. E. Costley, *Infrared*

- Phys.* **19**, 437 (1979).
- <sup>9</sup>K. Sakai and L. Genzel, *Reviews of Infrared and Millimeter Waves 1* (Plenum, New York, 1983), p. 155.
- <sup>10</sup>A. Munir, N. Hamanaga, H. Kubo, and I. Awai, *IEICE Trans. Electron.* **E88-C**, 40 (2005).
- <sup>11</sup>I. Awai, *IEEE Microw. Mag.* **9**, 55 (2008).
- <sup>12</sup>J. Zhou, L. Zhang, G. Tuttle, T. Koschny, and C. M. Soukoulis, *Phys. Rev. B* **73**, 041101(R) (2006).
- <sup>13</sup>H. Tao, N. I. Landy, C. M. Bingham, Z. Zhang, R. D. Averitt, and W. J. Padilla, *Opt. Express* **16**, 7181 (2008).
- <sup>14</sup>W. Padilla, A. Taylor, and R. Averitt, *Phys. Rev. Lett.* **96**, 107401 (2006).
- <sup>15</sup>H.-T. Chen, W. J. Padilla, J. M. O. Zide, A. C. Gossard, A. J. Taylor, and R. D. Averitt, *Nature (London)* **444**, 597 (2006).
- <sup>16</sup>Z. Jakšić, O. Jakšić, Z. Djuric, and C. Kment, *J. Opt. A, Pure Appl. Opt.* **9**, S377 (2007).
- <sup>17</sup>T. Kondo, T. Nagashima, and M. Hangyo, *Jpn. J. Appl. Phys., Part 2* **42**, L373 (2003).
- <sup>18</sup>M. Hangyo, M. Tani, and T. Nagashima, *Int. J. Infrared Millim. Waves* **26**, 1661 (2005).
- <sup>19</sup>S. Heavens, *Optical Properties of Thin Solid Films* (Butterworths, London, 1955).
- <sup>20</sup>I. Lee, S. Cho, S. H. Park, A. J. Heeger, C.-W. Lee, and S.-H. Lee, *Nature (London)* **441**, 65 (2006).
- <sup>21</sup>I. Lee, A. J. Heeger, and Y. Cao, *Phys. Rev. B* **48**, 14884 (1993).
- <sup>22</sup>I. Lee, L. R. Menon, C. O. Yoon, and A. J. Heeger, *Phys. Rev. B* **52**, 4779 (1995).
- <sup>23</sup>B. Chapman, R. G. Buckley, N. T. Kemp, A. B. Kaiser, D. Beaglehole, and H. J. Trodahl, *Phys. Rev. B* **60**, 13479 (1999).
- <sup>24</sup>A. B. Kaiser, *Adv. Mater.* **13**, 927 (2001).
- <sup>25</sup>OptiFDTD 7, Optiwave, 2007.
- <sup>26</sup>G. Gallot, S. E. Jamison, R. W. McGowan, and D. Grischkowsky, *J. Opt. Soc. Am. B* **17**, 851 (2000).
- <sup>27</sup>R. Mendis and D. Grischkowsky, *Opt. Lett.* **26**, 846 (2001).
- <sup>28</sup>D. J. Park, S. B. Choi, Y. H. Ahn, F. Rotermund, I. B. Sohn, C. Kang, M. S. Jeong, and D. S. Kim, *Opt. Express* **17**, 12493 (2009).
- <sup>29</sup>M. A. Seo, H. R. Park, S. M. Koo, D. J. Park, J. H. Kang, O. K. Suwal, S. S. Choi, P. C. M. Planken, G. S. Park, N. K. Park, Q. H. Park, and D. S. Kim, *Nature Photonics* **3**, 152 (2009).
- <sup>30</sup>H. T. Miyazaki and Y. Kurokawa, *Phys. Rev. Lett.* **96**, 097401 (2006).
- <sup>31</sup>H. T. Miyazaki and Y. Kurokawa, *Appl. Phys. Lett.* **89**, 211126 (2006).
- <sup>32</sup>Y. Kurokawa and H. T. Miyazaki, *Phys. Rev. B* **75**, 035411 (2007).
- <sup>33</sup>N. Murazawa, K. Ueno, V. Mizeikis, S. Juodkazis, and H. Misawa, *J. Phys. Chem. C* **113**, 1147 (2009).
- <sup>34</sup>K. Ueno, S. Juodkazis, T. Shibuya, Y. Yokota, V. Mizeikis, K. Sasaki, and H. Misawa, *J. Am. Chem. Soc.* **130**, 6928 (2008).
- <sup>35</sup>V. S. Cherkassky, B. A. Knyazev, V. V. Kubarev, G. N. Kulipanov, G. L. Kuryshv, A. N. Matveenko, A. K. Petrov, V. M. Popik, M. A. Scheglov, O. A. Shevchenko, and N. A. Vinokurov, *Nucl. Instrum. Methods Phys. Res. A* **543**, 102 (2005).
- <sup>36</sup>T. Idehara, T. Saito, I. Ogawa, S. Mitsudo, Y. Tatematsu, and S. Sabchevski, *Thin Solid Films* **517**, 1503 (2008).
- <sup>37</sup>J. Hebling, K.-L. Yeb, M. C. Hoffmann, B. Bartal, and K. A. Nelson, *J. Opt. Soc. Am. B* **25**, B6 (2008).